

Orientation Distributions for Cytochrome *c* on Polar and Nonpolar Interfaces by Total Internal Reflection Fluorescence

Andrey Tronin,* Ann M. Edwards,* Wayne W. Wright,[†] Jane M. Vanderkooi,[†] and J. Kent Blasie*

*Chemistry Department and [†]Department of Biochemistry and Biophysics, University of Pennsylvania, Philadelphia, Pennsylvania 19104 USA

ABSTRACT The formation of chemisorbed monolayers of yeast cytochrome *c* on both uncharged polar and nonpolar soft surfaces of organic self-assembled monolayers (SAM) on solid inorganic substrates was followed in situ by polarized total internal reflection fluorescence. Two types of nonpolar surfaces and one type of uncharged polar surface were used. The first type of nonpolar surface contained only thiol endgroups, while the other was composed of a mixture of thiol and methyl endgroups. The uncharged polar surface was provided by the mixture of thiol and hydroxyl endgroups. The thiol endgroups were used to form a covalent disulfide bond with the unique surface-exposed cysteine residue 102 of the protein. The mean tilt angle of the protein's zinc-substituted porphyrin was found to be 41° and 50° for the adsorption onto the nonpolar and uncharged polar surfaces, respectively. The distribution widths for the pure thiol and the thiol/methyl and thiol/hydroxyl mixtures were 9°, 1°, and 18°, respectively. The high degree of the orientational order and good stability achieved for the protein monolayer on the mixed thiol/methyl endgroup SAM makes this system very attractive for studies of both intramolecular and intermolecular electron transfer processes.

INTRODUCTION

Vectorially oriented single monolayers of the individual proteins, and bimolecular complexes thereof, participating in biological electron transfer reactions are very attractive for detailed biophysical studies of the correlation between the structures and the rates of intermolecular electron transfer in real biological systems. Such vectorially oriented monolayers, together with the development of appropriate techniques used for their assembly including the fabrication of supramolecular complexes, also provide for the possibility of biotechnological applications.

Vectorially oriented monolayers of yeast cytochrome *c* (YCC) can be formed via covalent binding of the protein's surface-exposed cysteine 102 residue to a specifically prepared soft organic surface, which includes thiol endgroups. The structures of such monolayers have been studied by x-ray interferometry/holography (Chupa et al., 1994), polarized X-ray absorption fine structure spectroscopy and optical linear dichroism (Edwards et al., 2000), and neutron interferometry (Kneller et al., 2001). These studies have shown that the structure within the monolayer is generally consistent with the known molecular structure of the protein given the location of the surface cysteine residue used to tether the protein to the soft organic surface. The utilization of covalent chemisorption via the unique surface cysteine to produce a particular vectorial orientation of the protein is very promising because there is the possibility of mutagenic substitution of some other surface residues by cysteine, thus changing the orientation of the protein with respect to the

soft surface. Techniques for the manipulation of the protein orientation with respect to the monolayer plane, together with reliable methods for structural characterization of these single monolayer systems, are essential for electron transfer studies. As shown by electrochemical surface-enhanced resonance Raman spectroscopy (Dick et al., 2000), the electron-transfer reaction between ferricytochrome *c* and a silver electrode strongly depends not only on the heme-electrode distance, but also on the heme orientation. Thus, to study the orientational dependence of the electron transfer, the protein monolayer used should be highly oriented, i.e., the orientational distribution should be narrow, stable, and well-characterized. Although the orientation of the covalently bound cytochrome is mainly determined by the location of the tethering residue on its surface, it also depends on the physicochemical properties of the substrate's soft organic surface. Linear dichroism measurements and molecular dynamics computer simulations have shown that the average (or mean) heme tilt angles of the YCC bound to either a nonpolar or an electrically neutral uncharged polar surface are different by several degrees (Edwards et al., 2000; Nordgren et al., submitted for publication). It is conceivable that the distribution width also depends on the physical properties of the substrate's soft alkylated surface, which would make one type of surface more favorable than another.

We report a study of the orientation distributions in YCC monolayers covalently bound to the soft surfaces of organic self-assembled monolayers (SAM) on solid inorganic substrates, the soft surface being either macroscopically nonpolar or uncharged-polar in nature. Chemisorption of a protein is also generally accompanied by a nonspecific binding, so a subsequent rinsing procedure was used to remove the nonspecifically bound protein. To investigate the possible influence of the rinsing procedure on the de-

Submitted July 2, 2001, and accepted for publication October 12, 2001.

Address reprint requests to Dr. A. Tronin, Chemistry Department, University of Pennsylvania, Philadelphia, Pennsylvania 19104. Tel.: 215-573-5609; Fax: 215-573-2112; E-mail: tronin@sas.upenn.edu.

© 2002 by the Biophysical Society

0006-3495/02/02/0996/08 \$2.00

terminated orientation distribution, we used three steps of rinsing of different duration and detergent content, and measured the peptide orientation in situ after each step. We also did measurements *ex situ*, where the buffer was substituted by humid air. The purpose of these measurements was to provide a reference for related x-ray structural studies using x-ray energies in the vicinity of the iron absorption edge, ($\sim 6\text{--}8\text{ KeV}$), which are facilitated by a humid atmosphere, as opposed to bulk water.

To characterize the orientation distribution of the protein, we used polarized total internal reflection fluorescence (PTIRF). In this technique, the orientation of the porphyrin is investigated by measuring the polarization of the fluorescence excited by an electric field directed normal to and along the monolayer surface. The main advantage of fluorescence measurements over other linear optical techniques is that fluorescence, a "two photon" process, makes it possible to determine two parameters of the orientation distribution assumed to be a simple Gaussian function, namely the mean tilt angle of the porphyrin (θ_m), and the width of the distribution (σ). The θ angle is defined as the angle between the normal to the porphyrin ring and the normal to the soft surface. This feature is of particular importance for biological applications because protein ultrathin films are usually not well-oriented. In many cases knowledge of the mean angle alone has no useful meaning, because for a very broad distribution, the width may be more important than the mean value. For many applications, however, even a rough estimate of the distribution width is useful, making it possible to characterize the quality of the monolayer film. PTIRF has been successfully used to study orientation distributions of various porphyrin-containing organic and bioorganic single-monolayer systems, such as adsorbed tetramethylpyridinium porphyrin (TMPyP) and porphyrin cytochrome *c* (Bos and Kleijn, 1995), covalently bound zinc porphyrin YCC (Edmiston and Saavedra, 1998), Langmuir monolayers of a dihelical synthetic peptide BBC16 containing Zn(II)protoporphyrinIX and mixed monolayers of dipalmitoylphosphatidic acid (DPPA), methyl palmitate (PME), and TMPyP (Tronin et al., 2000, 2001).

MATERIALS AND METHODS

Fluorescence measurements

In this section we outline only the experimental technique and data treatment procedure; the complete detailed description has been provided elsewhere (Tronin et al., 2000).

In polarized total internal reflection fluorescence, fluorophores are excited by an evanescent field, which appears in the optically sparse medium in immediate proximity to the interface, with an optically dense medium upon total internal reflection in the latter. The evanescent field can be polarized by choosing the polarization of the incident beam either parallel or perpendicular to the plane of incidence.

The experimental setup is shown in Fig. 1. The light beam, with a value of $\lambda = 514\text{ nm}$ from an argon laser, was directed to the axis of a two-circle Huber rotation stage. The sample holder was mounted on the inner rotation

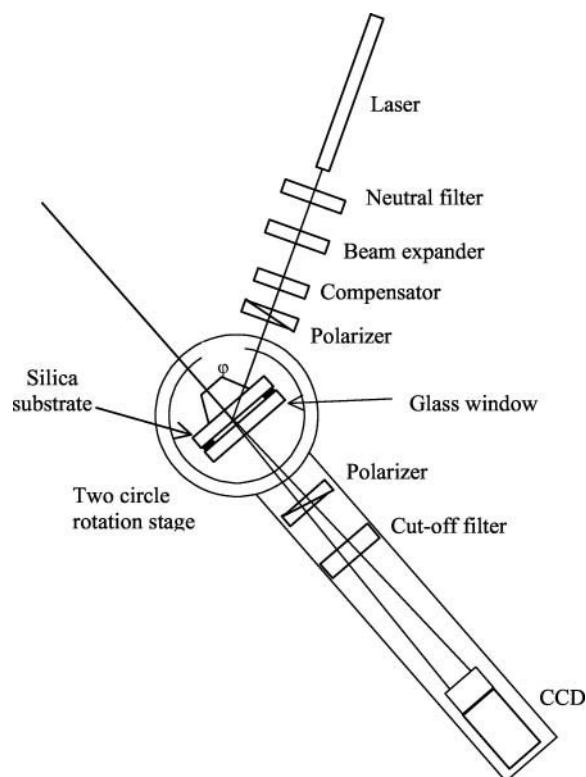


FIGURE 1 Experimental setup. See text for description.

axes and the detector rail was mounted on the outer circle. Rotation of the inner circle made it possible to change the incidence angle of the total internal reflection, while rotation of the outer circle was used to keep the detector setup perpendicular to the film surface. The laser output power was 20 mW. Before striking the coupling prism, the beam passed through a 0.6 neutral filter (Melles-Griot, Irvine, CA), a cylindrical expander, a quarter wave compensator (Melles-Griot), and a Glan-Thompson polarizing prism (Melles-Griot). The expander was used to increase the beam cross-section in vertical direction so that the beam footprint on the acquisition area was almost $1 \times 1\text{ cm}^2$. Such a large area was needed to increase the overall fluorescence output signal. The compensator was used to produce circularly polarized light before the linear polarizer so that the electric field components parallel and perpendicular to the plane of incidence in the beam incident on the air-prism interface were equal each other. The detection path contained a cutoff filter, a Glan-Thompson polarizing prism, and the detector. The wavelength cutoff was 570 nm (Melles-Griot). Excitation and emission polarizers were aligned by zeroing the beam passing through them. For this purpose the detector stage was rotated 90° and the sample holder was removed so that the detector saw the direct laser beam. The accuracy of the crossed polarizers position was $>15'$. Fluorescence was observed with a CCD camera (TE/CCD-512-TK by Princeton Instruments, Trenton, NJ, cooled to -40°C) through an F 28-mm lens (Nikon), with a collection angle of $<5^\circ$. A CCD has an advantage of directly imaging the illuminated spot, enabling the discrimination of the stray light and significantly reducing the background. This feature is of especially great help when viewing very weak fluorescent signals from single monolayer specimens. The beam was directed into the fused silica substrate with the help of a fused silica 60° dove prism. To enhance optical contact, refractive index matching liquid (Cargille Laboratories) was used. The flow cell was composed of the substrate, covered by a glass window of the same size as the substrate, and a rubber gasket. The angles of total internal reflection (ϕ) used were 85.5° , 70° , and 66° when the flow cell was

filled with buffer (wet measurements) and 85.5°, 60°, and 43.7° when the cell was filled with humid air (humid measurements).

By changing excitation/emission polarizations, fluorescence intensities I_{sx} , I_{sy} , I_{px} , I_{py} , (where the indices p, s indicate the polarization of the incident beam and x, y indicate the polarization of the emitted field) were acquired. Although the fluorescence intensities were stable and did not show significant decay with time, the acquisition at each excitation angle was repeated four times in the alternating reversed order, i.e., I_{sx} , I_{px} , I_{py} , I_{sy} , I_{sy} , I_{py} , I_{px} , I_{sx} , etc., to improve statistics and to eliminate the influence of porphyrin photobleaching.

The determination of the orientation parameters was done by minimization of the target function composed of the discrepancies between the calculated and measured intensities. The model for the calculation was based on two reasonable assumptions:

First, distribution of the angle θ obeys a simple Gaussian law,

$$P(\theta) = \frac{\exp(-(\theta - \theta_m)^2/2\sigma^2)}{\int_0^\pi \exp(-(\theta - \theta_m)^2/2\sigma^2)d\theta}$$

Second, the protein monolayer is axially symmetric about the normal to the monolayer plane on the macroscopic level (scale of the acquisition area).

We also took into account that the porphyrin dipoles were embedded in the monolayer, whose index of refraction was different from both the silica substrate and external medium. As a result, the normal component of the effective excitation field in the monolayer is lower than it is in the external medium by the factor of ϵ_f/ϵ_m , where ϵ_f and ϵ_m are the dielectric constants of the monolayer and external medium, respectively. For the former, we assume the value of 2.25 (refractive index 1.5), which is typical for protein films. With these assumptions, the dependence of the polarized fluorescence intensities on the mean tilt angle and the distribution width takes the form (Tronin et al., 2000):

$$\begin{aligned} I_{sy} &= CA_y^2 \left[\frac{3}{8} t(1 + I_4) + \frac{1}{4} (u + q)I_2 \right] \\ I_{py} &= \frac{C}{2} A_z^2 (\epsilon_m/\epsilon_f)^2 [u(1 - I_2) + t(I_2 - I_4)] \\ &\quad + CA_x^2 \left[\frac{1}{8} t(1 + I_4) + \frac{3}{4} (u - q)I_2 \right] \\ I_{sx} &= CA_y^2 \left[\frac{1}{8} t(1 + I_4) + \frac{3}{4} (u - q)I_2 \right] \\ I_{px} &= \frac{C}{2} A_z^2 (\epsilon_m/\epsilon_f)^2 [u(1 - I_2) + t(I_2 - I_4)] \\ &\quad + CA_x^2 \left[\frac{3}{8} t(1 + I_4) + \frac{1}{4} (u + q)I_2 \right] \end{aligned} \quad (1)$$

where

$$\begin{aligned} t &= \sin^2\varphi \sin^2(\varphi + \delta) + \cos^2\varphi \cos^2(\varphi + \delta) \\ q &= \sin\varphi \sin(\varphi + \delta) \cos\varphi \cos(\varphi + \delta) \\ u &= \sin^2\varphi \cos^2(\varphi + \Delta) + \cos^2\varphi \sin^2(\varphi + \delta) \end{aligned}$$

and

$$\begin{aligned} I_2(\theta_m, \sigma) &= \frac{\int_0^\pi \cos^2\theta \exp\left(-\frac{(\theta - \theta_m)^2}{2\sigma^2}\right) \sin\theta d\theta}{\int_0^\pi \exp\left(-\frac{(\theta - \theta_m)^2}{2\sigma^2}\right) \sin\theta d\theta} \\ I_4(\theta_m, \sigma) &= \frac{\int_0^\pi \cos^4\theta \exp\left(-\frac{(\theta - \theta_m)^2}{2\sigma^2}\right) \sin\theta d\theta}{\int_0^\pi \exp\left(-\frac{(\theta - \theta_m)^2}{2\sigma^2}\right) \sin\theta d\theta} \end{aligned}$$

where φ is the porphyrin rotation angle; δ is the angle between absorbing and emitting dipoles in the porphyrin ring; A_x , A_y , and A_z are the evanescent field components, which can be found in the classic book of Harrick (1967); and the multiplicative constant C incorporates all common factors such as excitation power, fluorescence yield, detector sensitivity, etc.

Measurements at different angles of incidence were used to test the validity of the optical model for the monolayer and the data treatment procedure. The variation of the incident angle provided different ratios of the evanescent field components, and thus of the measured fluorescent intensities. The recovered porphyrin orientation parameters should be independent of the incident angle, and any variation of these parameters would have indicated some inadequacy of our model including, among other things, the value for the refractive index of the protein monolayer or some errors in the data treatment.

Cytochrome c monolayer preparation

The YCC monolayers were formed by adsorption from an aqueous solution onto the soft surface of organic self-assembled monolayers (SAMs). The fused silica substrates were cleaned and the SAMs were formed via chemisorption onto their hard surface according to the procedure described previously (Xu et al., 1993). We used two types of nonpolar and one type of uncharged polar soft surfaces. The first type of nonpolar surface was produced by self-assembly of 11-trichlorosilylundecyl thioacetate (TTA), which provided a protected thiol-endgroup surface. The second one was formed by a 6:1 mole ratio of dodecyltrichlorosilane (DTS) and TTA, which provided a mixed methyl- and protected thiol-endgroup surface. The polar surface was produced using a 6:1 mole ratio of trichlorosilylacetoxundecane (TAOU) and TTA, which provided a mixed protected hydroxyl- and protected thiol-endgroup surface. The DTS was purchased from Hüls (Piscataway, NJ), TTA and TAOU were synthesized according to the procedure described elsewhere (Wasserman et al., 1989; Edmiston et al., 1997). The protecting groups were removed via acid hydrolysis by immersing the alkylated substrate in a 50:50 mixture of methanol and concentrated hydrochloric acid for 1.5 h. The contact angles with water were 87, 125, and 70° for SH-, SH/CH₃-, and SH/OH- terminated SAMs, respectively. By being alkylated in this way substrates were assembled into the flow cell, and the latter was lined up in the fluorometer. The flow cell was filled with the 10 μ M solution of the protein, zinc-substituted YCC from *Saccharomyces cerevisiae* in 1 mM TRIS, pH 8.0. The iron to zinc substitution in the protein porphyrin was performed as previously described (Vanderkooi et al., 1977). The protein exhibits a naturally occurring and unique cysteine residue 102 that would, therefore, be available for covalent disulfide bonding with the activated thiol endgroups of the SAM surface. The 6:1 mole ratio in the mixed SAMs was chosen so that on average, each thiol endgroup was surrounded by six methyl or hydroxyl

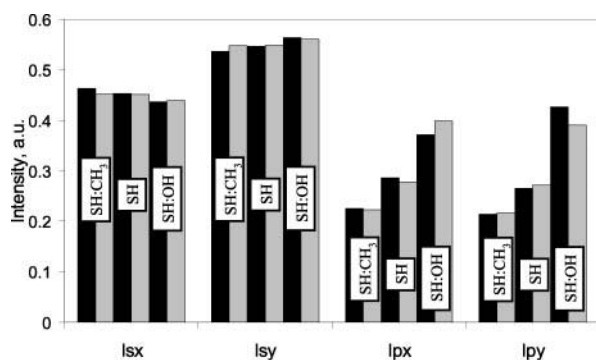


FIGURE 2 Fluorescence intensities for a YCC monolayer chemisorbed onto different soft SAM surfaces. *Black bars*: experiment; *gray bars*: calculation result for the best fit of the orientation parameters θ_m and σ . All measurements shown were performed with an excitation angle of 70° .

endgroups and thus isolated on the SAM surface. The so-alkylated substrates were incubated for 4 h, then the protein solution was removed and the flow cell flushed with TRIS buffer for 20 min. At this time the first fluorescent measurement was made, then the cell was flushed overnight and the second measurement was made. After that, the cell was flushed with RBS detergent solution (1 ml RBS in 500 ml TRIS) for 1 h and finally flushed with the buffer again for 1 h. At this time the third measurement was made. The buffer was then removed and the cell filled with air, which has been bubbled through water at room temperature, and the fourth measurement was made. The relative humidity of the air in the cell was 70%. We refer to these four measurements as “immediate wet,” “rinsed wet,” “detergent rinsed wet,” and “humid,” respectively. The monolayers of the nonsubstituted Fe-porphyrin YCC prepared otherwise identically were used for background scattering measurements.

RESULTS AND DISCUSSION

Results of a typical “detergent rinsed wet” measurement of the YCC monolayer chemisorbed to the different SAM soft surfaces are shown in Fig. 2. Black, dark gray, and light gray bars correspond to the SH/CH₃, pure SH-, and SH/OH-terminated SAMs, respectively. The hatched bars to the right of each solid filled bar show the calculation result for the best fit of the orientation parameters θ_m and σ . All measurements shown were performed with the excitation angle of 70° . One can see reasonably good agreement between the experimental data and calculations. The discrepancies are within experimental errors of the measured intensities. The discrepancies are somewhat higher for the

polar surface; however, the experimental errors were also different, dependent on the SAM type used. For both types of nonpolar surface the errors were $<0.6\%$, whereas for the uncharged polar surface the errors were twice as large. Because all experimental conditions were otherwise identical, and the overall absolute fluorescence intensity was essentially of comparable magnitude for every type of SAM, the difference in the errors can be attributed to a lower stability of the protein monolayer on the uncharged polar SAM, resulting in the larger variations of the measured intensities. The absolute fluorescence intensity levels decreased with the rinsing of the monolayer. The most pronounced difference was between “immediate wet” and “rinsed wet” measurements, while successive detergent rinsing resulted in very little change. The decrease between “immediate wet” and “rinsed wet” depended also on the type of SAM surface used. It was higher in the case of a nonpolar surface, especially for the pure SH-terminated SAM (where the nonpolar nature presumably arises from the dimerization of neighboring thiol endgroups not involved in the covalent tethering of the protein to the SAM surface). This fact indicates that the nonspecific adsorption to the nonpolar surface is higher, which is not unexpected for a membrane protein. The fact that the intensity does not decrease with successive rinsing shows that only the covalently bound protein molecules remained on the surface to form the monolayer. The monolayer coverage of the YCC on SH/CH₃ SAM achieved after the detergent rinsing was also confirmed by the optical absorption measurements (Edwards et al., 2000) and our attenuated total reflection measurements (unpublished results) on the same system.

The results of the orientation distribution parameters determination are summarized in Table 1. The results for the “rinsed wet” and “detergent rinsed wet” were nearly identical, so they are presented in the same column. For the nonpolar surfaces the mean tilt angle is $\sim 41\text{--}44^\circ$, whereas for the uncharged polar surface it is noticeably higher, $\sim 50^\circ$. The distribution is very narrow for the SH/CH₃ SAM, demonstrating a high degree of orientational order within the protein monolayer in this case. The worst orientational order is for the uncharged polar surface, in which case the distribution width is $\sim 18^\circ$. As a result of the higher errors in the measured parameters, the uncertainty of the

TABLE 1 Orientation distribution parameters of the YCC monolayer on different SAM soft surfaces and at different stages of the monolayer preparation

Surface Termination	Immediate Wet		Rinsed Wet and Detergent Rinsed Wet		Humid
	Mean Tilt (Deg)	Dispersion (deg)	Mean tilt (deg)	Dispersion (deg)	Mean tilt (deg)
Pure SH	44.7 ± 1	6.7 ± 4	43.4 ± 1	9.3 ± 5	40.2 ± 2
SH/CH ₃ = 1:6	44.8 ± 2	0.8 ± 0.1	41.3 ± 1	1.1 ± 0.9	30.0 ± 12.0
SH/OH = 1:6	50.5 ± 1	3.8 ± 3	50.0 ± 0.5	18 ± 15	50.9 ± 10

See text for details.

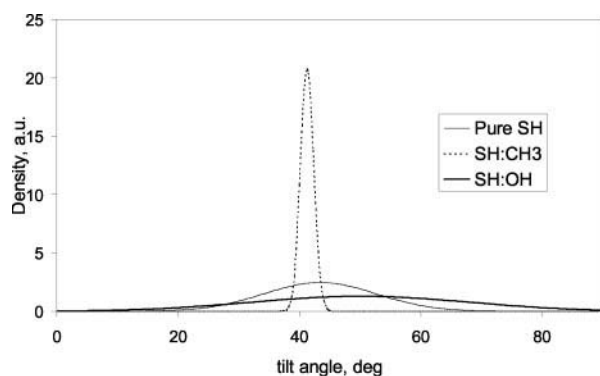


FIGURE 3 Porphyrin orientation distribution for YCC monolayers on different SAM surfaces as determined from the PTIRF measurements.

orientational distribution parameters determined, especially σ , is much higher for the polar SAM. The Gaussian orientational distributions for the parameters of the “rinsed wet” monolayers are given in Fig. 3.

Changing from “wet” to “humid” environments produces almost no change for the pure SH and uncharged polar SAMs. For the SH/CH₃ SAM there is a decrease in the mean tilt angle; however, its uncertainty in the “humid” measurement is very high, and the difference between “wet” and “humid” is within the error range. Because of the poor accuracy of the “humid” measurements we were not able to determine the distribution width in this case, and thus it is not given in Table 1. The errors were high in the “humid” measurement because of the high level of the background scattering, which increases with the optical contrast at the interface. For the “wet” measurements the background scattering was in the order of 3–4% of the fluorescence intensity, whereas for the “humid” measurements it was typically ~15–25%. Although the background scattering has been measured from the Fe-YCC monolayers, some minor differences in the sample alignment and monolayer structure may play a more significant role in the case of “humid” measurement, producing higher errors.

After rinsing in detergent, the overall fluorescence intensity for SH- and SH/OH-terminated SAMs was about the same, while for the SH/CH₃ SAM it was 1.5 times higher, meaning that the protein surface coverage for this SAM was also higher by the same amount. At least three conclusions follow from these observations:

1. There is a significant degree of dimerization of the SH-termini in the case of pure SH SAM, consistent with its macroscopic polarity, because the affinity toward the protein of this substrate is lower than that of the SH/CH₃-terminated SAM;
2. Besides the engineered SAM surface chemistry and cysteine residue location on the YCC surface, which determine the orientation of the chemisorbed protein, the macroscopic polarity of the surface rather than the mono-

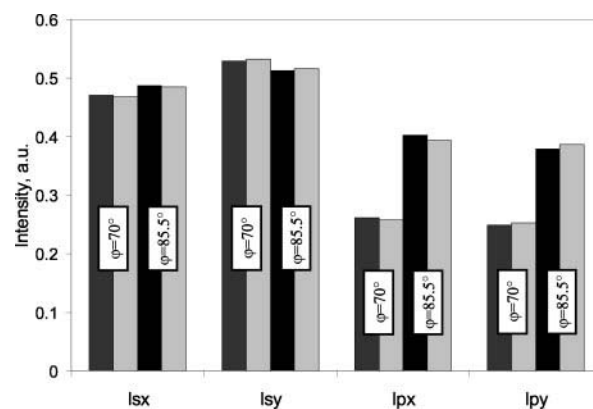


FIGURE 4 Fluorescence intensities for a YCC monolayer chemisorbed onto SH/H₃ SAM for different excitation angles. *Black bars*: experiment; *gray bars*: calculation result for the best fit of the orientation parameters θ_m and σ . The resulting values for the orientation parameters were found to be $\theta_m = 43.2^\circ$, $\sigma = 1.0^\circ$ for $\varphi = 70^\circ$; and $\theta_m = 41.8^\circ$, $\sigma = 0.8^\circ$ for $\varphi = 85.5^\circ$.

layer coverage (or in-plane density) affects the mean tilt angle of the protein monolayer. The mean tilt angle was quite different for two surfaces with different polarity and about the same protein density, namely the pure SH- and SH/OH-terminated SAMs, whereas for nonpolar SAMs, namely pure SH- and SH/CH₃-SAMs with different monolayer densities, the mean tilt angle was essentially the same;

3. Distribution width is probably determined by both the surface polarity and protein monolayer density, as there appears to be a gradual decrease of σ with the change from polar to nonpolar surface and increase of surface density.

The measurements at different excitation angles φ were used to verify the validity of the data treatment procedure. The typical results of the “rinsed wet” measurements at two different angles of the total internal reflection are shown in Fig. 4. As it is clearly seen, the ratios of the intensities are quite different at different angles due to the differences in the evanescent field components. The resulting values for the orientation distribution parameters were found to be essentially the same, being $\theta_m = 43.2^\circ$, $\sigma = 1.0^\circ$ for $\varphi = 70^\circ$; and $\theta_m = 41.8^\circ$, $\sigma = 0.8^\circ$ for $\varphi = 85.5^\circ$. The critical angle for the total internal reflection at the fused silica/water interface is 65.57° , so the values of φ utilized are almost as far apart as experimentally achievable. The fact that the found values for the orientation distribution parameters were essentially the same for these different excitation angles proves the correctness of the data treatment procedure.

It was shown (Tronin et al., 2001) that the mean tilt and the distribution width as determined by polarized fluorescence are highly interrelated, and the accuracy of the orientation distribution determination is given by some range of (θ_m, σ) values, which comply with the fluorescence

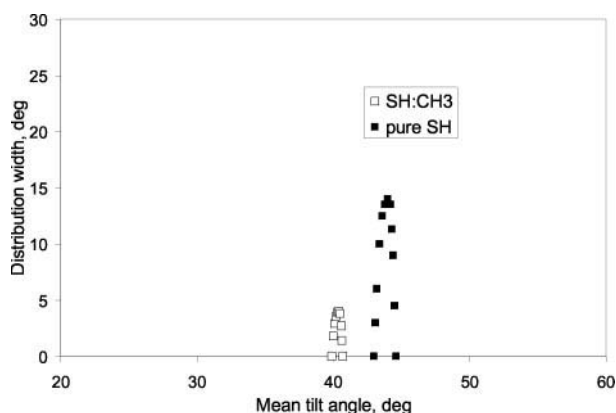


FIGURE 5 Uncertainty of the (θ_m, σ) determination for YCC monolayers on the nonpolar SAMs. *Filled squares*: pure SH-terminated surface; *empty squares*: SH/CH₃-terminated surface. The region of possible (θ_m, σ) values is limited by the shown curve and the lines $\theta_m = 90^\circ$ and $\sigma = 90^\circ$. Uncertainty is due to errors in the measurement of the fluorescence intensities.

intensities. To find this range we analyze the target function. This function is, by definition, the sum of the squared discrepancies between measured and calculated intensities. This means that all values of the orientation angles, which produce discrepancies lower than experimental errors, are experimentally indistinguishable. The loci of θ_m and σ that satisfy this condition are enclosed by intersection of the target function with the plane $Z = (\text{Err}_{sx}^2 + \text{Err}_{sy}^2 + \text{Err}_{px}^2 + \text{Err}_{py}^2)$.

These regions of allowed distribution parameters are shown in the Fig. 5 (nonpolar SAMs) and Fig. 6 (uncharged polar SAM). For the nonpolar surfaces the mean tilt angle and distribution width are confined to small regions, with $41^\circ < \theta_m < 42^\circ$ and $0^\circ < \sigma < 14^\circ$ for the pure -SH SAM

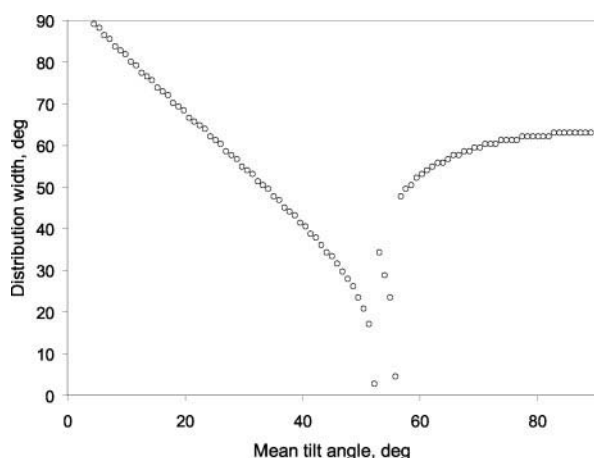


FIGURE 6 Uncertainty of the (θ_m, σ) determination for YCC monolayers on the uncharged-polar SAM. The region of possible (θ_m, σ) values is limited by the shown curve and the lines $\theta_m = 90^\circ$ and $\sigma = 90^\circ$. Uncertainty is due to errors in the measurement of the fluorescence intensities.

and for the SH/CH₃ mixed SAM, the width is even narrower, $\sim 5^\circ$. For the polar surface the region of the allowed θ_m and σ becomes very broad, in both the mean tilt and width with $10^\circ < \theta_m < 90^\circ$ and $0^\circ < \sigma < 90^\circ$. There are several reasons for such a high coupling of the orientation parameters in the latter case. The first is already mentioned above due to the higher level of the experimental errors. The second is that the values of the orientation parameter lie in the unfavorable range for their determination. As was shown previously (Tronin et al., 2000), the possibility to resolve the parameters θ_m and σ depends on their values, strongly diminishing when the tilt angle approaches the “magic-angle” value, which is $\sim 54^\circ$, and when the distribution becomes broad. This is exactly the case for the uncharged polar surface.

The orientation distribution parameters for the nonpolar surfaces are in excellent agreement with the published results (Edmiston and Saavedra, 1998) of the TIRF study of a very similar system, which also consisted of the YCC monolayer covalently tethered to the SAM surface via a disulfide bond, although the -SH-terminated surface in that study was prepared in a different way.

There is disagreement between the results presented here and the earlier optical linear dichroism measurements of the same systems performed in our group (Edwards et al., 2000). In that paper the values of 59° and 62° for the nonpolar and uncharged polar SAM cases, respectively, were reported. Although these earlier results were obtained with Fe-porphyrin YCC, we believe that the present PTIRF measurements utilizing Zn-porphyrin YCC are more accurate due to the following reasons, although the coordination of Fe-porphyrin and Zn-porphyrin in YCC may be different, giving rise to the apparent discrepancy (see paragraph below). First of all, by using linear dichroism one cannot assess the distribution width, and the mean tilt angle is determined on the assumption that the distribution is infinitely sharp, which per se represents a flaw in the optical model used. The other reason is the poorer accounting for the background absorption. The best estimation of the background for the linear dichroism measurement can be done by using a blank substrate without an adsorbed protein monolayer, which may be not sufficient, especially given very low optical density of the heme in the YCC monolayer.

It is also interesting to compare our experimental data with the results of the molecular dynamics computer simulations of the YCC molecule covalently tethered to these SAM soft surfaces (Nordgren et al., submitted for publication; Tobias et al., 1996). In the paper by Nordgren and co-workers a number of different external conditions for the YCC/SAM system were considered, two of them particularly relevant for the present study:

1. YCC molecule covalently tethered via a disulfide bond to either the nonpolar or uncharged polar surface, surrounded by 500 water molecules. The iron atom in the

heme was 6-coordinate, with four in-plane nitrogen ligands from the porphyrin, the fifth axial nitrogen ligand from a histidine residue and the sixth axial sulfur ligand from methionine residue;

The same conditions as above, except that the sixth heme iron sulfur ligand was “switched off”, i.e., unbound.

The authors referred to these conditions as “nonpolar or polar wet” and “nonpolar or polar nosulfur,” respectively. For the “wet” conditions on the polar SAM the authors presented results for two systems, which differ in their initial configurations. The first one, “polar wet,” was obtained starting from the fully equilibrated “nonpolar wet” protein/SAM structure, then simply changing the polarity of the SAM endgroups and continuing the trajectory to equilibration. The other, referred to as “polar crystalline,” was obtained starting from the same initial configuration as the “nonpolar wet” case. Thus, we consider it more appropriate to compare our experimental results with the “nonpolar wet” and “polar crystalline” cases because they share the precise initial configuration. Tobias et al. (1996) considered the same YCC/SAM system, but without water; these cases were later referred to as “nonpolar or polar dry” in Nordgren et al. Under these conditions the authors calculated the mean (time-averaged) heme tilt angle and the deviation of the protein C α backbone conformation of the x-ray crystal structure. The deviation over the length of the peptide was quantified as an “RMSDX” value.

“Nonpolar wet” conditions produced the mean tilt angle of 53.7°, whereas for “polar-crystal” the tilt was appreciably higher, 61.9°. In the “nosulfur” conditions the tilt angle was 48.4°, and 60.0° for the nonpolar and polar SAMs, respectively. Although there is a certain discrepancy in absolute values between our results and the MD simulations, the difference in the tilt angle for the polar and nonpolar cases agrees reasonably well with our experimental results. The shift of the tilt angle toward lower values in “nosulfur” conditions, which diminishes the discrepancy with the experimental data, suggests that the zinc atom in the porphyrin has only five ligands. Although there is some controversy in the literature concerning the zinc atom coordination in the YCC porphyrin (Anni et al., 1995; Ye et al., 1997), the five-coordinate model appears to be more likely (Ye et al., 1997).

The strongest effect of the SAM’s surface polarity on the mean tilt angle appears in the simulations for the “dry” conditions, where $\theta_m = 36^\circ$ for the nonpolar surface and $\theta_m = 66^\circ$ for polar one. We observed a similar tendency in the “wet” to “humid” measurements for SH/CH₃ and SH/OH terminated SAMs, where the difference in mean tilt angle increased from $\theta_m = 5\text{--}9^\circ$ to $\theta_m \approx 20^\circ$.

The difference in the water content of the experimental protein monolayer systems and the model systems investigated could also account for some discrepancy in mean

heme tilt angles observed in the experiments and molecular dynamics simulations. In fact, the water content in the experimental close-packed protein monolayer is probably larger than the value used in “wet” models (namely 500 water molecules per 1 YCC molecule is only ~20% that of bulk water for the monolayer simulated that was not close-packed). Neutron interferometry (e.g., Kneller et al., 2001) is now being used to directly determine the water content of these protein monolayer systems under the variety of experimental hydration conditions described here. In fact, the water/cytochrome *c* mole ratios were found to be in the range of 150–300:1 for relative humidities of 80–90% for the nonpolar and uncharged polar SAM cases. Under our “humid” conditions with 70% relative humidity, the actual water content may be substantially less than that, making this case possibly more close to the “dry” case in the MD simulations.

The large change of the mean tilt angle from “wet” to “humid” conditions for the nonpolar SAM can be attributed to the protein conformational change. While the RMSDX value was found to be essentially the same for the polar and nonpolar SAMs in “wet” conditions, in “damp” conditions it changed by 12% for nonpolar SAM and only by 2% for polar SAM. For “dry” conditions the change was 55% and 41%, respectively, again relatively higher for the nonpolar case. For “wet” conditions the protein conformation was the same for both surfaces, which means that the difference in porphyrin tilt angle observed in our study for “wet polar” and “wet nonpolar” is due to the protein reorientation.

CONCLUSIONS

The vectorial orientation of Zn-porphyrin yeast cytochrome *c* (YCC) molecules covalently tethered via a disulfide linkage to thiol endgroups on the soft surface of a SAM depends on the overall macroscopic polarity of the SAM endgroup surface. The mean tilt angle of the porphyrin ring with respect to the monolayer plane was found to be ~41° and 50° for the nonpolar and uncharged polar surfaces, respectively. These values agree reasonably well with the YCC molecular structure, given the tethering cysteine residue 102 used, and with molecular dynamics simulations reported in the literature (Nordgren et al., submitted for publication; Tobias et al., 1996). For the nonpolar SAM case, these results agree very well with reported experimental results for a similar YCC monolayer (Edmiston and Saavedra, 1998). The highest degree of orientational order was obtained in the monolayers formed on the nonpolar SAM surfaces composed of mixed SH/CH₃ endgroups. PTIRF measurements show that the orientation distribution is very narrow in this case, σ being <2°. For the uncharged polar surface the orientational order is much poorer, $\sigma = 18^\circ \pm 15^\circ$, although the errors are necessarily much larger in this case. The PTIRF technique was shown to be adequate for studying the orientation distribution of the protein mono-

layers. In future studies we are planning to apply the same technique to explore the possibility of gaining control over the vectorial orientation of the YCC molecules within such tethered single monolayers by changing the location of the tethering cysteine residue on the protein's surface via site-directed mutagenesis.

This work was supported by National Institutes of Health Grants GM 33525 and GM48130.

REFERENCES

- Anni, H., J. M. Vanderkooi, and L. Mayne. 1995. Structure of zinc-substituted cytochrome *c*: nuclear magnetic resonance and optical spectroscopic studies. *Biochemistry*. 34:5744–5753.
- Bos, M. A., and L. M. Kleijn. 1995. Determination of the orientation distribution of adsorbed fluorophores using TIRF. II. Measurements on porphyrin and cytochrome *c*. *Biophys. J.* 68:2573–2578.
- Chupa, J. A., J. P. McCauley, Jr., R. M. Strongin, A. B. Smith III, J. K. Blasie, L. J. Peticolas, and J. C. Bean. 1994. Vectorially oriented membrane protein monolayers: profile structures via x-ray interferometry/holography. *Biophys. J.* 67:336–348.
- Dick, L. A., A. J. Haes, and R. P. Van Duyne. 2000. Distance and orientation dependence of heterogeneous electron transfer: a surface enhanced resonance Raman scattering study of cytochrome *c* bound to carboxylic acid terminated alkanethiols adsorbed on silver electrodes. *J. Phys. Chem. B*. 104:11752–11762.
- Edmiston, P. L., J. E. Lee, S.-S. Cheng, and S. S. Saavedra. 1997. Molecular orientation distributions in protein films. I. Cytochrome *c* adsorbed to the substrates of variable chemistry. *J. Am. Chem. Soc.* 119:560–570.
- Edmiston, P. L., and S. S. Saavedra. 1998. Molecular orientation distributions in protein films. III. Yeast cytochrome *c* immobilized on pyridyl disulfide-capped phospholipid bilayers. *Biophys. J.* 74:999–1006.
- Edwards, A. M., K. Zhang, C. E. Nordgren, and J. K. Blasie. 2000. Heme structure and orientation in single monolayers of cytochrome *c* on polar and nonpolar soft surfaces. *Biophys. J.* 79:3105–3117.
- Harrick, N. J. 1967. *Internal Reflection Spectroscopy*. Interscience Publishers, New York.
- Kneller, L. R., A. M. Edwards, C. E. Nordgren, J. K. Blasie, N. F. Berk, S. Krueger, and C. F. Majkrzak. 2001. Hydration state of single cytochrome *c* monolayers on soft interfaces via neutron interferometry. *Biophys. J.* 80:2248–2261.
- Tobias, D. J., W. Mar, J. K. Blasie, and M. L. Klein. 1996. Molecular dynamics simulations of a protein on hydrophobic and hydrophilic surfaces. *Biophys. J.* 71:2933–2941.
- Tronin, A., J. Strzalka, X. Chen, P. L. Dutton, and J. K. Blasie. 2000. Determination of the porphyrin orientation distribution in Langmuir monolayers by polarized epifluorescence. *Langmuir*. 16:9878–9886.
- Tronin, A., J. Strzalka, X. Chen, P. L. Dutton, B. M. Ocko, and J. K. Blasie. 2001. Orientational distributions of the di- α -helical synthetic peptide ZnPPIX-BBC16 in Langmuir monolayers by x-ray reflectivity and polarized epifluorescence. *Langmuir*. 17:3061–3066.
- Vanderkooi, J. M., R. Landsberg, G. W. Hayden, and C. S. Owen. 1977. Metal-free and metal-substituted cytochromes *c*. Use in characterization of the cytochrome *c* bindings sites. *Eur. J. Biochem.* 81:338–347.
- Wasserman, S. R., H. Biebuyck, and G. M. Whitesides. 1989. Monolayers of 11-trichlorosilylundecyl trioacetate: a system that promotes adhesion between silicon dioxide and evaporated gold. *J. Mater. Res.* 4:886–892.
- Xu, S., R. F. Fischetti, J. K. Blasie, L. J. Peticolas, and J. C. Bean. 1993. Profile and in-plane structures of self-assembled monolayers on Ge/Si multilayer substrates by high resolution x-ray diffraction employing x-ray interferometry/holography. *J. Phys. Chem.* 97:1961–1969.
- Ye, S., T. Cotton, and N. M. Kostic. 1997. Characterization of zinc-substituted cytochrome *c* by circular dichroism and resonance Raman spectroscopic methods. *J. Inorg. Biochem.* 65:219–226.